THE JOURNAL OF PHYSICAL CHEMISTRY C

Comment

pubs.acs.org/JPCC

Comment on "Oxygen Vacancy Ordering and Electron Localization in CeO_2: Hybrid Functional Study"

M. Verónica Ganduglia-Pirovano,*[,†] Gustavo E. Murgida,[‡] Valeria Ferrari,[‡] and Ana María Llois[‡]

[†]Instituto de Catálisis y Petroleoquímica of the Consejo Superior de Investigaciones Científicas, 28049 Madrid, Spain

[‡]Centro Atómico Constituyentes, GIyA, CNEA, San Martín, Buenos Aires, Argentina and Consejo Nacional de Investigaciones Científicas y Técnicas, C1033AAJ Buenos Aires, Argentina

J. Phys. Chem. C **2016**, *120* (25), 13325−13331. DOI: 10.1021/acs.jpcc.6b00865

J. Phys. Chem. C **2017**, *121*, DOI: 10.1021/acs.jpcc.7b02945

Supporting Information

Han et al. have recently published an article[1] on the ordering of oxygen vacancies and electron localization in bulk CeO_2 using density functional theory (DFT) with the Heyd−Scuseria−Ernzerhof (HSE06) functional.[2−4] On the basis of their results, they concluded that oxygen vacancies tend to linearly order in the [111] CeO_2 direction with a weakened excess charge localization compared with the case of a single vacancy. Moreover, distinct vacancy-induced lattice relaxations were found to be crucial for the interpretation of their results. This Comment is written to prevent misconceptions regarding the localization of the excess charge and the associated lattice relaxations discussed in the work of Han et al.[1]that misses any citation to previous recent work[5−7] on related subjects using the DFT+*U* approach with the Perdew−Becke−Ernzerhof (PBE) functional.[8] As an example, Han et al.[1] describe the case of an isolated bulk vacancy and claim that the two excess electrons left behind upon vacancy formation localize on two nearest-neighbor Ce^{4+} cations that are reduced to Ce^{3+}. Moreover, for the cases of a third-neighbor vacancy pair (VV3) and vacancy line along the [111] direction, their results indicate a homogeneous distribution of the Ce^{3+} ions on nearest-neighbor sites to the vacancies; namely, each vacancy has two first cationic Ce^{3+} neighbors. It is astonishing that they get such results because with DFT(PBE)+*U* the second-neighbor cationic sites to an isolated vacancy are preferred,[5−7] and the distribution of first-neighboring Ce^{3+} to vacancy pairs is predicted to be inhomogeneous.[7] The consistency between both the DFT(PBE)+*U* and DFT(HSE06) approaches for describing the electronic structure of partially reduced ceria and for predicting energy differences between different Ce^{3+} distributions is well documented.[7,9] Here we used exactly the same DFT(HSE06)-based methodology[10] and computational code (VASP)[11] as Han et al.[1] and reconsidered the cases of isolated vacancies, VV3 vacancy pairs, and lines along the [111] direction in bulk CeO_2. From our point of view, their study suffers from a number of critical flaws. The main issues are (I) not having investigated in detail many possible configurations of the Ce^{3+} ions and (II) the reproducibility and correctness of their calculated defect structures. These aspects are vital for the interpretation of their results, as outlined in the following sections.

I. EXCESS CHARGE LOCALIZATION

I.a. Isolated Vacancy. The first goal is to clarify the above-mentioned apparent discrepancy between Han et al.'s[1] DFT(HSE06)-based results with respect to the excess charge localization for isolated vacancies in bulk CeO_2 as compared with previous DFT(PBE)+*U*-based works in the literature.[5−7] Therefore, we created one oxygen vacancy and applied DFT(HSE06) to different Ce^{3+} configurations for the two excess electrons, which are denoted *n*N−*m*N, where *n* and *m* correspond to the *n*th and *m*th cationic neighboring shells to the defect, respectively. In particular, we considered the 1N−1N configuration as well as a 2N−2N with a distance between the Ce^{3+} ions equal to that of first-neighbors in the Ce sublattice, which corresponds to the lowest-energy 2N−2N configuration with DFT(PBE)+*U*.[5−7] Table 1 lists the calculated vacancy formation energies. Contrary to the conclusions of Han et al.,[1] the 2N−2N configuration with Ce^{3+} away from the vacant site clearly exhibits a lower formation energy, with both the DFT(PBE)+*U* approach and the HSE06 functional providing consistent results.

Table 1. Vacancy Formation Energy (E_v) (in eV/atom) for an Isolated Vacancy in Bulk Ceria [$Ce_{32}O_{63}$] for Different Ce^{3+} Configurations[a]

Ce^{3+} position	Ce^{3+}−Ce^{3+}	E_v	
		DFT+*U*[b]	HSE06
1N−1N	1N	2.91	3.79
2N−2N	1N	2.85	3.74

[a] *n*N−*m*N indicates a pair of Ce^{3+} ions in the *n*th and *m*th cationic neighboring shells to the defect. The closest distance between Ce^{3+} ions (Ce^{3+}−Ce^{3+}) is given as *n*th neighbors (*n*N) in the Ce sublattice. [b] U = 4.5 eV.

Although Han et al.[1] missed providing any calculated defect formation energy, which we find rather unusual for a theoretical paper on the topic of oxygen vacancies in bulk ceria, they should have at least mentioned and discussed results in the literature in the context of their topic. We note that the isolated

Received: February 23, 2017
Published: August 29, 2017

Table 2. Vacancy Formation Energy (E_v) (in eV/atom) for VV3 Pairs in Bulk Ceria [$Ce_{32}O_{62}$] for Different Ce^{3+} Configurations and Corresponding Vacancy−Vacancy Interaction Energies (E_{int}) (in eV) with HSE06 Using Two Different References for the Isolated Defect (cf. Table 1)

	Ce^{3+} position		E_v		E_{int}	
label[a]	Vac_1	Vac_2	DFT+U[b]	HSE06	Vac_{1N-1N}	Vac_{2N-2N}
$VV3_{22-22}$	1N−1N	1N−1N	2.90	3.79	−0.01	+0.10
$VV3_{22-21}$	1N−1N	1N−1N	2.88			
$VV3_{22-13}$	1N−1N	1N−1N	2.85			
$VV3_{22-03}$	1N−1N	1N−1N	2.85			
$VV3_{22-12}$	1N−1N	1N−1N	2.83			
$VV3_{22-02}$	1N−1N	1N−1N	2.82	3.71	−0.17	−0.06
$VV3_{31-13}$	3×1N	1×1N	2.77	3.65	−0.28	−0.18
$VV3_{40-13}$	4×1N	0	2.86	3.75	−0.10	+0.01
$VV3_{00-02}$	2N−2N	2N−2N	2.93	3.82	+0.06	+0.16

[a] Ce^{3+} configurations are labeled as $VV3_{AB-ab}$, where A and B are the numbers of Ce^{3+} ions first neighbors to each vacancy, a is the number of Ce^{3+} on the [111] direction, and b is the number (up to 3) of intersecting {110} planes that contain Ce^{3+} ions. [b] U = 4.5 eV

Table 3. Vacancy Formation Energy (E_v) (in eV/atom) for Four Linear Vacancies in Bulk Ceria [$Ce_{32}O_{60}$] for Different Ce^{3+} Configurations

	Ce^{3+} position				E_v	
label[a]	Vac_1	Vac_2	Vac_3	Vac_4	DFT+U[b]	HSE06
$Line_{2222-03}$	1N−1N	1N−1N	1N−1N	1N−1N	3.09	3.99
$Line_{2222-02}$	1N−1N	1N−1N	1N−1N	1N−1N	3.06	3.97
$Line_{3131-03}$	3×1N	1×1N	3× 1N	1×1N	3.05	3.95

[a] Ce^{3+} configurations are labeled as $Line_{ABCD-ab}$, where A, B, C, and D are the numbers of Ce^{3+} ions first neighbors to each vacancy, a is the number of Ce^{3+} on the [111] direction, and b is the number (up to 3) of intersecting {110} planes that contain Ce^{3+} ions. [b] U = 4.5 eV

vacancy is used as reference for the calculation of the interaction energy between vacancies forming pairs, as discussed below.

I.b. Vacancy Pairs and Lines along [111]. Having made clear the case of a single vacancy, we examined next the case of two-third-neighbor vacancies (VV3) forming a pair without a Vac-Ce-Vac bridge along the [111] direction. Han et al.[1] found that a VV3 pair with homogeneously distributed Ce^{3+} ions, that is, with both vacancies having two nearest-neighbor Ce^{3+} [2×(1N−1N)], was the most stable divacancy structure. Furthermore, they calculated the vacancy−vacancy interaction within vacancy pairs as $E_{int} = E(Ce_{32}O_{62}) + E(Ce_{32}O_{64}) - 2E(Ce_{32}O_{63})$, where $E(Ce_{32}O_{62})$, $E(Ce_{32}O_{63})$, and $E(Ce_{32}O_{64})$ are the total energies of the defective bulk with one and two vacancies and of the perfect bulk crystal, respectively. Using the 1N−1N configuration of the isolated vacancy as reference, which according to them was the lowest-energy structure, the vacancy−vacancy interaction within the most stable VV3 pair was found to be significantly attractive with $E_{int} \approx 0.2$ eV.

We have first used DFT(PBE)+U and considered all six possible VV3 pairs with [2×(1N−1N)] configuration and selected VV3 structures with less homogeneous Ce^{3+} distributions with, for example, one vacancy having three and the other having only one nearest-neighbor Ce^{3+} (cf. Table 2). Later, DFT(HSE06) was selectively employed to confirm the DFT(PBE)+U prediction that a VV3 structure with a nonhomogeneous [3×1N, 1×1N] Ce^{3+} distribution is more stable than the lowest energy [2×(1N−1N)] structure by ∼0.1 eV (cf. $VV3_{31-13}$ and $VV3_{22-02}$ in Table 2). The investigation of all possible configurations for the four excess electrons is beyond the intention of this Comment and is a formidable task. Here we just want to stress how important the electron localization is for determining the lowest energy structure that Han et al.[1] apparently failed to obtain.

The calculation of the interaction energy between vacancies in VV3 pairs will depend not only on the particular VV3 structure but also on the isolated vacancy configuration used as reference. As mentioned above, Han et al.[1] compared a [2×(1N−1N)]-type VV3 structure with the [1N−1N] single vacancy configuration and found an attractive interaction of ∼0.2 eV, which we can reproduce (cf. $VV3_{22-02}$ in Table 2). However, considering the most stable [2N−2N] single-vacancy configuration as reference, the vacancy−vacancy interaction within such a VV3 pair becomes barely attractive. Instead, we found that it is the interaction between vacancies within a VV3 pair with a nonhomogeneous [3×1N, 1×1N] Ce^{3+} distribution, the one that is considerably attractive ($E_{int} \approx -0.2$ eV, cf. $VV3_{31-13}$ in Table 2). Thus Han et al.[1] got the right result about the [111] direction being a possible direction for vacancy clustering but for the wrong reasons, and the nonconsideration of the lowest-energy single- and divacancy structures renders their interpretations questionable. We also note that Han et al.[1] neglected to mention works in the literature[7,12,13] that suggested the possibility of ordering of second- and third-neighbor vacancies in bulk CeO_2 along the [110] and [111] directions, respectively.

Finally, we also considered a few Ce^{3+} distributions for the case of four vacancies aligned in the [111] direction, where two of them correspond to having two $VV3_{22-02}$ or $VV3_{31-13}$ consecutive VV3 pairs (cf. Table 2). In line with the results discussed above, the linear structure with a nonhomogeneous Ce^{3+} distribution, with two vacancies having three and the other two having only one nearest-neighbor Ce^{3+}, is more stable than the one with homogeneously distributed Ce^{3+} by ∼50 meV (cf. $Line_{3131-03}$ and $Line_{2222-02}$ in Table 3). We note that Han et al.[1] discussed a linear structure of the homogeneous type as the most stable. As pointed out above, the discussion of the issue of the lowest-energy excess charge distribution for a given vacancy

DOI: 10.1021/acs.jpcc.7b01800
J. Phys. Chem. C 2017, 121, 21080−21083

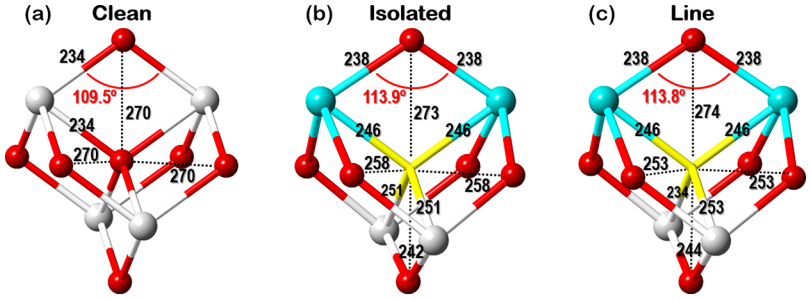

Figure 1. Lattice relaxations around vacancies in bulk CeO_2. (a) Clean, (b) isolated V_{1N-1N}, and linear $Line_{2222-02}$ structures. Ce^{3+}, Ce^{3+}, and O atoms are depicted in cyan, white, and red, respectively. The position of the vacancy is shown in yellow. Selected interatomic distances are given in pm.

arrangement is complicated by the fact that numerous configurations have to be considered. Notwithstanding this difficulty, special attention has to be given to the fate of the electrons left behind upon vacancy formation in ceria-based compounds because the system's properties, such as geometry and electronic structure, do depend on it.

II. LATTICE RELAXATIONS

It is well known that oxygen vacancy-induced lattice relaxations in ceria are crucial to the localization of the excess charge.[7,9,14] Han et al.[1] reported peculiar lattice relaxations in their calculated vacancy structures that constituted the basis for discussing the origin and nature of the vacancy-induced gap states and suggesting variations in the magnetic superexchange interactions between two neighboring Ce^{3+} cations through a nonmagnetic anion. As discussed above, they considered vacancy structures with homogeneously distributed Ce^{3+} ions and suggested that the $Ce^{3+}-O-Ce^{3+}$ angles are 107, 110, and 121° for an isolated vacancy, a VV3 pair, and a vacancy line in the [111] direction, respectively. The corresponding Ce−O−Ce angle in the clean structure (a_0 = 5.40 Å) is 109.5°. It is well known that upon vacancy formation in ceria the Ce atoms that are first neighbors to the defect move away from the vacant site, and the O atoms that are also first neighbors to the defect within the oxygen sublattice move toward the vacant site.[7,9,14,15] In our view, given the expected atom displacements, a smaller or practically unchanged $Ce^{3+}-O-Ce^{3+}$ angle for the single vacancy and VV3 vacancy pair, compared with the clean structure, cannot be explained. To shed light on this issue, we inspected our calculated isolated V_{1N-1N}, $VV3_{22-02}$, and $Line_{2222-02}$ structures that should be directly comparable with those discussed by Han et al.[1] Figure 1 shows the mentioned relaxations away (by about 0.1 to 0.2 Å) and toward the vacant site (by about 0.1 to 0.3 Å) of neighboring Ce and O atoms, respectively, for the examples of the $VV3_{22-02}$ and $Line_{2222-02}$ structures. These relaxation effects are crucial to the larger Ce−O−Ce angles formed by the Ce atoms within the first coordination shell to the vacancy compared with the nondefective structure. In particular, the $Ce^{3+}-O-Ce^{3+}$ angle increases from 109.5 to 113.9° and 113.8° in the isolated V_{1N-1N} and $Line_{2222-02}$ structures, respectively. Moreover, we found that as the vacancy concentration increases from 1/64 (isolated) to 1/16 (line) the $Ce^{3+}-O-Ce^{3+}$ angle barely changes.

In brief, the key findings of the Han et al.[1] study cannot be reproduced, and thus their conclusions are questionable. We hope the community finds this Comment useful for providing additional understanding of how important electron localization in reduced ceria systems is and helpful for preventing misconceptions.

■ ASSOCIATED CONTENT

Supporting Information

The Supporting Information is available free of charge on the ACS Publications website at DOI: 10.1021/acs.jpcc.7b01800.

Coordinates of the calculated isolated vacancy, VV3 pairs, and vacancy lines structures with HSE06. (PDF)

■ AUTHOR INFORMATION

Corresponding Author

*E-mail: vgp@icp.csic.es.

ORCID

M. Verónica Ganduglia-Pirovano: 0000-0003-2408-8898

Notes

The authors declare no competing financial interest.

■ ACKNOWLEDGMENTS

We thank ANPCyT (Grant No. PICT-1555), CONICET-Argentina (Grant No. PIP-0069), and MINECO Spain (CTQ2012-32928 and CTQ2015-71823-R) for financial support. Computer time provided by the CESGA, BSC, University of Cantabria-IFCA, and BIFI-ZCAM and support from the COST Action CM1104 is gratefully acknowledged.

■ REFERENCES

(1) Han, X.; Amrane, N.; Zhang, Z.; Benkraouda, M. Oxygen Vacancy Ordering and Electron Localization in CeO_2: Hybrid Functional Study. *J. Phys. Chem. C* **2016**, *120*, 13325−13331.

(2) Heyd, J.; Scuseria, G. E.; Ernzerhof, M. Hybrid Functionals Based on a Screened Coulomb Potential. *J. Chem. Phys.* **2003**, *118*, 8207.

(3) Heyd, J.; Scuseria, G. E.; Ernzerhof, M. Erratum: Hybrid Functionals Based on a Screened Coulomb Potential [J. Chem. Phys. 118, 8207 (2003)]. *J. Chem. Phys.* **2006**, *124*, 219906.

(4) Krukau, A. V.; Vydrov, O. A.; Izmaylov, A. F.; Scuseria, G. E. Influence of the Exchange Screening Parameter on the Performance of Screened Hybrid Functionals. *J. Chem. Phys.* **2006**, *125*, 224106.

(5) Kullgren, J.; Hermansson, K.; Castleton, C. Many Competing Ceria (110) Oxygen Vacancy Structures: From Small to Large Supercells. *J. Chem. Phys.* **2012**, *137*, 044705.

(6) Allen, J. P.; Watson, G. W. Occupation Matrix Control of d- and f-Electron Localisations Using DFT+U. *Phys. Chem. Chem. Phys.* **2014**, *16*, 21016−21031.

(7) Murgida, G. E.; Ferrari, V.; Ganduglia-Pirovano, M. V.; Llois, A. M. Ordering of Oxygen Vacancies and Excess Charge Localization in Bulk Ceria: A DFT+U Study. *Phys. Rev. B: Condens. Matter Mater. Phys.* **2014**, *90*, 115120.

DOI: 10.1021/acs.jpcc.7b01800
J. Phys. Chem. C 2017, 121, 21080−21083

(8) Perdew, J.; Burke, K.; Ernzerhof, M. Generalized Gradient Approximation Made Simple. *Phys. Rev. Lett.* **1996**, *77*, 3865−3868.
(9) Murgida, G. E.; Ganduglia-Pirovano, M. V. Evidence for Subsurface Ordering of Oxygen Vacancies on the Reduced CeO_2(111) Surface Using Density-Functional and Statistical Calculations. *Phys. Rev. Lett.* **2013**, *110*, 246101.
(10) We considered a (2 × 2× 2) supercell of the conventional cubic cell with $Ce_{32}O_{64}$ composition with calculated lattice constant (a_0 = 5.40 Å).[16] The Kohn−Sham equations were solved using the projected augmented wave (PAW) method, and for Ce and O atoms, the (5s, 5p, 6s, 4f, 5d) and (2s, 2p) states, respectively, were treated as valence with a plane-wave cutoff energy of 400 eV. The Brilloiun zone was sampled using a (2 × 2 × 2) Monkhorst-Pack grid.
(11) *VASP.5.3.5*, http://www.vasp.at.
(12) Hull, S.; Norberg, S.; Ahmed, I.; Eriksson, S.; Marrocchelli, D.; Madden, P. Oxygen Vacancy Ordering within Anion-Deficient Ceria. *J. Solid State Chem.* **2009**, *182*, 2815−2821.
(13) Gopal, C. B.; van de Walle, A. Ab Initio Thermodynamics of Intrinsic Oxygen Vacancies in Ceria. *Phys. Rev. B: Condens. Matter Mater. Phys.* **2012**, *86*, 134117.
(14) Ganduglia-Pirovano, M.; Da Silva, J.; Sauer, J. Density-Functional Calculations of the Structure of Near-Surface Oxygen Vacancies and Electron Localization on CeO_2(111). *Phys. Rev. Lett.* **2009**, *102*, 026101.
(15) Murgida, G.; Vildosola, V.; Ferrari, V.; Llois, A. Charge Localization in Co-Doped Ceria with Oxygen Vacancies. *Solid State Commun.* **2012**, *152*, 368−371.
(16) Da Silva, J.; Ganduglia-Pirovano, M.; Sauer, J.; Bayer, V.; Kresse, G. Hybrid Functionals Applied to Rare-Earth Oxides: The example of Ceria. *Phys. Rev. B: Condens. Matter Mater. Phys.* **2007**, *75*, 045121.

DOI: 10.1021/acs.jpcc.7b01800
J. Phys. Chem. C 2017, 121, 21080−21083